Novel endogenous engineering platform for robust loading and delivery of functional mRNA by extracellular vesicles

Antje Maria Zickler*[,1,#], Xiuming Liang*[,1,2,#], Mariacristina De Luca[3,4], Dhanu Gupta[1,5], Giulia Corso[1,6], Lorenzo Errichelli[3], Justin Hean[3], Noriyasu Kamei[1,7], Zheyu Niu[1,8], Guannan Zhou[1,9], Samantha Roudi[1], Joel Nordin[1], Virginia Castilla-Llorente[3], Samir EL Andaloussi[1,#]

[1] Biomolecular Medicine, Department of Laboratory Medicine, Karolinska Institutet, Stockholm, Sweden
[2] Cancer Research Laboratory, Shandong, University-Karolinska Institutet collaborative Laboratory, School of Basic Medical Science, Shandong University, Jinan, China
[3] Evox Therapeutics Ltd., Oxford, United Kingdom
[4] Human Technopole, Milan, Italy
[5] Department of Paediatrics, University of Oxford, Oxford, United Kingdom
[6] Evercyte GmbH, Vienna, Austria
[7] Laboratory of Drug Delivery Systems, Faculty of Pharmaceutical Sciences, Kobe Gakuin University, Kobe, Japan
[8] Department of Hepatobiliary Surgery, Shandong Provincial Hospital Affiliated to Shandong First Medical University, Jinan, China
[9] Department of Gynecology, The Obstetrics and Gynecology Hospital of Fudan University, Shanghai, China
* These authors contributed equally to this work.
[#] Corresponding authors.
Email: antje.zickler@ki.se; xiuming.liang@ki.se; samir.el-andaloussi@ki.se

ABSTRACT

Messenger RNA (mRNA) has emerged as an attractive therapeutic molecule for a range of clinical applications. For *in vivo* functionality, mRNA therapeutics require encapsulation into effective, stable, and safe delivery systems to protect the cargo from degradation and reduce immunogenicity. Here, we developed a bioengineering platform for efficient mRNA loading and functional delivery using naturally-derived nanoparticles, Extracellular Vesicles (EVs). By expressing the highly specific PUFe RNA-binding domain fused to CD63 in EV producer cells stably expressing the target mRNA, our system exceeds mRNA loading efficiencies by up to 4.5-fold over previously reported EV-based approaches. By combining with an mRNA-stabilizing protein, PABPc, and a fusogenic endosomal escape moiety, VSVg, functional mRNA delivery *in vivo* is achieved at doses substantially lower than clinically used lipid nanoparticles. Our technology solves substantial drawbacks currently associated with EV-based nucleic acid delivery systems and could enable new applications for mRNA therapeutics.

INTRODUCTION

Nucleic acid-based therapeutics, in particular messenger RNA (mRNA), have played a pivotal role in recent developments of RNA-based vaccination platforms[1] or cancer immunotherapy[2]. Furthermore, mRNA has emerged as an attractive molecule for the development of precision medicine approaches, such as protein-replacement therapy, gene editing, and genomic engineering[3-7].
The major limitation to the delivery of mRNA therapeutics pertains to their instability and inherent inability to bypass the lipid bilayer of cells[8]. Thus, they need to be packaged into

nanoparticles to ensure cargo protection and efficient delivery into the cytoplasm of target cells[8]. Current state-of-the-art for therapeutic mRNA delivery is the encapsulation into synthetic nanoparticles, such as lipid nanoparticles (LNPs). Although their efficacy is indisputable for the delivery of mRNA-based SARS-CoV-2 vaccines for the prevention of coronavirus disease 2019 (COVID-19)[9-11], their clinical applications are sometimes associated with adverse effects of different severities, including immunogenicity due to their synthetic nature[12-14]. Moreover, safe RNA delivery to organs other than the liver has proven to be very challenging using LNPs[8,15].

A relatively new nanotechnology-based approach is the use of engineered extracellular vesicles (EVs), including exosomes, for the delivery of mRNA therapeutics. EVs are lipid bilayer-enclosed, naturally secreted nanovesicles of 30-2000 nm in size[16]. EVs are immunologically tolerated and have the capacity to cross biological barriers to reach any tissue of the organism, including distant organs[17,18]. They contain macromolecular cargo from the source cell and are able to deliver these proteins, nucleic acids, or lipids to recipient cells[17,18]. Most importantly, they can be bioengineered to carry luminal therapeutic cargo as well as target molecules on their surface[17,18].

Incorporation of therapeutic mRNA cargo into pre-isolated EVs using exogenous loading approaches, such as co-incubation or electroporation, have been successfully applied previously[19,20]. However, they require large amounts of material, the loading is relatively inefficient, and thus they might not be sustainable in a clinical setting. Instead, endogenous loading approaches seem more suitable for the efficient loading of mRNA therapeutics of larger molecular sizes. Endogenous EV loading methodologies involve transient or permanent genetic engineering of the parental EV-producing cells to incorporate cargo into EVs during EV biogenesis. Mere overexpression of the target mRNA in producer cells leads to passive loading into the EVs, however, specific enrichment of the mRNA cargo in the EVs proves quite inefficient without an active loading strategy[21]. As certain proteins are naturally enriched in EVs, fusing specific proteins to these provides an effective mean to enrich for both therapeutic and targeting moieties on the surface and/or lumen of EVs[22-25]. In recent years, several studies have underpinned the importance of specific cellular engineering to actively load mRNAs into EVs for subsequent high efficiency delivery *in vivo*[26-28]. Cells are typically engineered with two different genetic constructs; one that expresses an EV sorting protein fused to an RNA binding domain (RBD), and another that expresses the mRNA of interest. Depending on the nature of the RBD, such as whether it recognizes a structural element or specific nucleotide sequences, corresponding interacting sites are inserted in the 3´UTRs of the mRNA (Targeted and Modular EV Loading (TAMEL) approach)[26].

Substantial drawbacks of current endogenous EV engineering strategies for mRNA loading include mRNA instability due to long artificial 3'UTRs, insufficient mRNA loading despite active EV sorting, as well as unsolicited carry-over of plasmid DNA that potentially interferes with the assessment of mRNA functionality[29-31]. To address these shortcomings, we developed a novel TAMEL-based platform for efficient mRNA delivery using engineered EVs. The central element to this system is a stably integrated target mRNA expression cassette in the genome of EV producer cells to convey robust batch-to-batch reproducibility of EV mRNA loading. As EV sorting scaffold, we engineered CD63, a tetraspanin abundantly expressed in EVs, fused to a high-affinity mammalian RBD. The target mRNA therefore carries repeats of the respective RBD recognition sequences in its 3'UTR. We identified an optimized version of the designer Pumilio and FBF homology domain, termed PUFe[32] as the lead candidate RBD by screening mRNA loading efficiencies of three PUF-derived RBDs[32-34] and a cleavage-deficient mutant of Cas6f[35]. The engineered EVs demonstrated efficient, robust, and reproducible mRNA cargo loading, outperforming previously published TAMEL-based mRNA loading approaches. For *in vivo* application, the EV producer cells were further engineered to express the mRNA-stabilizing protein PABPc, demonstrating for the first time the importance of mRNA stability for

efficient EV-mediated delivery. Importantly, using this engineering strategy produced EVs capable of extrahepatic mRNA delivery *in vivo* at doses as low as 20 ng per kg body weight, a dose which is at least an order of magnitude lower than those currently used with LNPs[36].

RESULTS

Generation of an EV-specific mRNA loading platform.

To achieve specific endogenous loading of engineered mRNA into EVs, we designed a two-component system for expression in EV producer cells. This approach combined an EV loading scaffold, i.e. an EV sorting domain fused to an RNA-binding domain (RBD) (Fig. 1a), with a co-expressed target mRNA containing multiple repeats of the RBD-dependent high-affinity motif in its 3'end (Fig. 1b). We fused an EV-sorting domain, the tetraspanin CD63, to either the bacteriophage MS2 coat protein (MCP) as published before[26], the non-cleaving S148A mutant of the CRISPR-associated protein Cas6f[35], or three engineered RBDs derived from the designer Pumilio and FBF homology domain (PUF)[32], PUFm, PUFe and PUFx2, respectively (Fig. 1a). PUFm was chosen for its very high affinity to the RNA target sequence ($K_d \approx 4$ pM)[34], PUFe was engineered to bind 8 nucleotides of low abundance in mammalian cells rendering it highly specific for the target RNA[32], and PUFx2 was designed to bind to a longer stretch of 16 target nucleotides[33]. Correspondingly, we engineered mRNA expression constructs with 6x high-affinity loops for MCP-binding as published[26], 6x hairpin structures for Cas6f (S148A) binding and 10x high-affinity motifs for binding to each PUF-derived RBD (Fig. 1b). MRNA expression constructs were designed for Nanoluciferase (Nanoluc or NL)[37], enhanced green fluorescent protein (eGFP), and Cre recombinase (Cre) reporter proteins, as well as murine Ox40L as functional protein.

Engineered EVs from cells with genomically integrated target mRNA-expression cassettes display high mRNA loading efficiencies.

Endogenously engineered EVs for therapeutic mRNA loading are often produced by transient co-transfection of multiple plasmids to overexpress engineering constructs in EV producer cells[27,38,39]. This approach has proven effective, yet awareness of the potential pitfalls, such as residual plasmid or transfection reagent in the EV preparation, is required when interpreting experimental results from EV cargo quantification and delivery assays[29-31]. Additionally, the inclusion of appropriate controls to account for passive loading of both target mRNA and the resulting protein is crucial to interpreting the loading and delivery correctly[21]. Here, HEK293T EV producer cells were engineered to stably express the target mRNA from a single genomic integration using the ϕC31 integrase system[40,41] (Fig. 2a). This approach allowed for the generation of mRNA-encoding plasmid-free EV preparations and ensured similar rates of passive loading. To evaluate mRNA loading efficiencies, EVs that were both actively loaded (target mRNA EVs) and passively loaded (target control EVs) were generated from the same stable cell line. For instance, Nanoluc mRNA EVs and control EVs were produced by transfection of stable cells expressing Nanoluc mRNA with a particular RBD binding motif with either the corresponding motif-compatible CD63-RBD or a non-binding incompatible CD63-RBD. Unless stated otherwise, CD63-MCP as RBD motif-incompatible control scaffold was used for all our generated constructs. With this approach we ensured that both mRNA EVs and control EVs derived from the same engineered producer cells and EV biogenesis setup.

First, we determined the mRNA loading capabilities of the novel EV scaffold constructs and tested them using Nanoluc mRNA with distinct 3'UTR RBD binding motifs. After EV isolation, the average particle diameter was verified by NTA for control as well as mRNA loaded EVs at 101 (± 2.6) nm (Supplementary Fig. S 1a) and confirmed CD63-RBD construct expression, Nanoluc protein expression, and reference protein expression in both EVs and producer cells by Western Blotting (Fig. 2b and Supplementary Fig. S 1b, respectively). Nanoluc protein

expression was further corroborated by luminescence measurements, which showed that the engineered cells producing mRNA-loaded EVs or control EVs contained similar amounts of Nanoluc protein from the genomically integrated mRNA construct (Supplementary Fig. S 1c), showcasing the benefit of the ϕC31 integrase system. Importantly, all EVs contained readily detectable quantities of passively loaded Nanoluc protein, yet without substantial differences between mRNA EV and respective control EV preparations (Fig. 2c).

Next, we assessed the performance in mRNA loading for the four novel CD63-RBD loading scaffolds. While the relative expression of Nanoluc mRNA in producer cells was similar in all samples with a maximum difference of 1.5-fold (Supplementary Fig. S 1d), the actively loaded mRNA EVs contained substantially more Nanoluc mRNA molecules than passively loaded control EVs as determined by absolute quantification using RT-qPCR (Fig. 1d). The enrichment over control values ranged from 18.5-fold for CD63-Cas6, to 65-fold for both PUFm and PUFx2, and reached more than 230-fold for CD63-PUFe (Fig. 2d). The superior performance of CD63-PUFe as EV mRNA loading platform was consistent over at least three independent experiments.

To assess the mRNA loading performance of CD63-PUFe in comparison to the published CD63-MCP-based mRNA loading platform[26], additional stable HEK293T EV producer cell lines expressing eGFP-PUFe$_{bind}$ mRNA, eGFP-MCP$_{bind}$ mRNA, mOx40L-PUFe$_{bind}$ mRNA, and mOx40L-MCP$_{bind}$ mRNA, respectively, were created. After validation of transgene expression by flow cytometry (Supplementary Fig. S 1e), we transfected the respective plasmid encoding the compatible CD63-RBD, i.e. either CD63-PUFe or CD63-MCP, and purified EVs as described previously. On average over three independent experiments, CD63-PUFe performed 1.7-fold (mOx40L mRNA), 2.5-fold (eGFP mRNA), and 4.3-fold (Nanoluc mRNA) better in actively loading mRNA into EVs than CD63-MCP (representative data shown in Fig. 1e).

In summary, we established a novel engineering approach for EV mRNA loading using stable target mRNA expression in EV producer cells, thereby avoiding the numerous drawbacks of transient expression of target mRNA from plasmid. Moreover, CD63-PUFe proved to function as a robust mRNA loading scaffold for EV bioengineering with superior performance in mRNA loading as compared to a previously established system. Thus, CD63-PUFe was selected as loading scaffold for all subsequent experiments.

EV-mediated mRNA delivery *in vitro*.

To evaluate the functionality of mRNA-loaded EVs as drug delivery vehicles, we first assessed the ability of naked EV-derived Nanoluc-PUFe$_{bind}$ mRNA to engage in translation. We transfected purified EV RNA into Huh7 and HEK293T recipient cells and measured Nanoluc protein activity at different time points (Fig. 3a and supplementary Fig. S 2a). While RNA from control EVs did not yield Nanoluc protein expression in transfected cells, RNA from Nanoluc mRNA EVs showed robust translation of Nanoluc protein *in vitro*.

Next, we performed EV uptake experiments to evaluate the release and translation of EV-encapsulated mRNA *in vitro*. First, Huh7 cells were treated with escalating doses of EVs actively loaded with Nanoluc mRNA or the particle-matched amount of passively loaded control EVs. After 24 h, treated cells were analyzed for Nanoluc protein activity. To account for Nanoluc protein not derived from mRNA translation, i.e. protein passively loaded into the EVs during biogenesis, the luminescence from EV-treated cells was normalized to the luminescence derived from the respective amount of EVs. An increase of this ratio in cells treated with Nanoluc mRNA EVs over control-treated cells provides a measure for the relative amount of Nanoluc protein resulting from mRNA translation. For all three doses, we observed higher ratios of Nanoluc protein from cells treated with Nanoluc mRNA EVs, indicating successful translation of delivered mRNA (Supplementary Fig. S 2b). Next, we investigated the accumulation of Nanoluc signal over time. For this, the uptake assay in Huh7 cells was

performed with a constant EV mRNA amount, 0.6 pg per $1x10^4$ cells, and Nanoluc protein activity was measured at different time points. To determine the rate of Nanoluc protein accumulation with and without supply from actively loaded Nanoluc mRNA, we normalized the values measured at the respective time points to the value measured at 2 h, when the signal should derive almost exclusively from passively loaded Nanoluc protein and the least amount of mRNA translation was expected (Fig. 3b). As control EVs only contained passively loaded Nanoluc protein as well as passively loaded Nanoluc mRNA, the rate of Nanoluc protein accumulation in cells treated with control EVs was considerably lower than in cells treated with Nanoluc mRNA EVs. Taken together, *in vitro* uptake experiments successfully demonstrated functional mRNA delivery via EVs.

Co-expression of PABPc stabilizes actively loaded EV mRNA.

The enrichment of Nanoluc mRNA in actively loaded EVs compared to control EVs was not reflected in the rate of Nanoluc protein expression upon EV delivery. This could be an indication of mRNA instability either during mRNA loading into EVs or during EV cargo delivery. To counteract this, further engineering of the EV producer cells was implemented. It was previously shown that the insertion of artificial sequences, such as MS2-binding arrays for the MS2-MCP system, into the 3'UTR of mRNAs can perturb their ability for efficient translation termination and, as a result, target them for nonsense-mediated decay (NMD)[42-44]. Thus, the introduction of repeated RNA-binding motifs into the 3'UTR of the target mRNA may foster mRNA instability in our system. Interestingly, PABPc, one of the main proteins involved in maintaining mRNA stability, binds to the polyA-tail of mRNA and thereby protects it from 3'UTR-directed degradation via the NMD pathway[45-47]. Therefore, to enhance general mRNA stability during EV production, EV producer cells were additionally engineered to co-express PABPc (Fig. 3c). EVs were harvested as previously described, average particle diameters were measured by NTA (110 ± 4.9 nm (mock), 119 ± 2.1 nm (PABPc), Supplementary Fig. S 3a), and PABPc expression was validated by Western Blot in both EVs and producer cells (Supplementary Fig. S 3b). As PABPc protects mRNA from degradation from the 3'UTR, we next investigated whether PABPc co-expression led to an increase in total RNA quantities in EVs and producer cells. Thus, we measured total RNA in defined amounts of cells and EVs and determined the relative enrichment upon PABPc co-expression. In producer cells, PABPc co-expression did not lead to an increase in total RNA amounts indicated by a PABPc/mock ratio around 1 in three different experiments (Supplementary Fig. S 3c). However, PABPc expression substantially enriched the harvested EVs in RNA as demonstrated by PABPc/mock ratios ranging from 3- to 14-fold irrespective of the CD63-RBD expression (Supplementary Fig. S 3c). Furthermore, Nanoluc-$PUFe_{bind}$ mRNA loading was substantially increased in Nanoluc mRNA EVs when PABPc was co-expressed (Fig. 3d). Taken together, these data suggest an overall stabilizing influence of PABPc co-expression on all mRNA in EVs and thus a potentially beneficial effect on the active loading of engineered mRNA. Next, the effect of PABPc-stabilized EV mRNA upon delivery to recipient cells was evaluated and EV uptake experiments were performed. Huh7 cells were treated for 24 h with mRNA-loaded EVs or control EVs, both produced either with or without PABPc co-expression. Cells treated with control or Nanoluc mRNA EVs carrying PABPc-stabilized mRNA showed higher signal than cells treated with respective EVs without PABPc (Supplementary Fig. S 3d). Interestingly, although the loading of mRNA into EVs strongly improved by expression of PABPc, the EV cargo delivery and rate of mRNA translation *in vitro* did not fully reflect the improved loading. However, co-expression of PABPc during EV production clearly suggested increased Nanoluc mRNA stability and was thus included in subsequent *in vivo* studies.

mRNA-loaded EVs show extrahepatic translation at low doses in mice.

The impact of EVs as biotherapeutic delivery agents *in vivo*, particularly concerning EV biodistribution and uptake into target tissues, is influenced by a variety of factors. These features are impossible to mimic *in vitro*. Thus, EV-mediated mRNA delivery may be more efficient *in vivo* than *in vitro*. To test this, we intravenously (iv) injected mice with mRNA-loaded EVs at an mRNA dose of 25 ng/kg body weight and sacrificed the mice at 1, 6, and 24 h post-injection to harvest organs and analyze the tissue for Nanoluc expression (Fig. 3e). We have previously reported that, without extra translation, the signal from EV-borne Nanoluc protein in tissue declines rapidly over 24 h[23]. In fact, signals across most tissues are negligible already after one hour when using Nanoluc laden EVs devoid of Nanoluc-encoding mRNA. As expected, we observed a decline in Nanoluc protein signal from liver and spleen lysates over the three analyzed time points. Intriguingly, in lysates from kidney and lung the signal did not decrease (Fig. 3e), which indicated the presence of replenished protein from mRNA translation.

To corroborate these findings, we repeated the experiment including control EVs. Nanoluc mRNA EVs at escalating mRNA doses, or particle-count-matched control EVs, respectively, were injected. The Nanoluc protein measurements in harvested mouse tissues were normalized to the respective signal in EVs to account for the co-delivery of passively loaded Nanoluc protein. We then determined the ratio of signal from mRNA animals to control animals for each organ, so that a value higher than 1 would indicate accumulated protein from mRNA translation (Fig. 3f). At an mRNA dose of 20-30 ng/kg body weight, translation was observed for all organs at 24 h post-injection. Interestingly, we observed a decline in relative signal for all four analyzed organs at 48 h post-injection, although apart from liver the ratio over control was still above 1. In contrast, at the higher dose of 50-60 ng/kg body weight, the signal at 48 h increased, strongly suggesting successful mRNA delivery and translation to extrahepatic organs at this mRNA dose. Taken together, we here demonstrated the feasibility of using engineered EVs as mRNA delivery vehicle *in vivo* at mRNA doses as low as 20 ng/kg body weight.

Co-expression of the fusogenic viral protein VSVg improves EV-mediated mRNA delivery *in vitro* and *in vivo*.

As observed *in vitro*, the protein translation rates from mRNA EVs did not correlate with their substantial enrichment in actively loaded mRNA molecules over control EVs. Thus, inefficiency in cargo release after EV uptake may be another major obstacle to mRNA delivery. To facilitate endosomal escape, we introduced the Vesicular Stomatitis Virus g (VSVg) protein, a viral fusion protein previously used to facilitate the delivery of EV cargo[26,48], to be expressed on the surface of both mRNA EVs and control EVs (Fig. 4a). After EV production, particle size (128 ± 5.4 nm (mock), 133 ± 6.8 nm (VSVg), Supplementary Fig. S 4a), VSVg expression by Western Blot (Supplementary Fig. S 4b) as well as mRNA loading (Supplementary Fig. S 4c) were analyzed. This was followed by testing the impact of VSVg co-expression on the uptake and release of the EVs *in vitro*. Huh7 cells were treated with mRNA EVs at a dose of 0.2 to 0.3 pg mRNA per $1x10^4$ cells or particle count-matched control EVs, both with and without VSVg expression, respectively, and analyzed 24 h later. In the presence of VSVg, a higher Nanoluc protein signal from recipient cell lysate for both cells treated with mRNA EVs or control EVs was observed, as compared to cells treated with EVs without VSVg (Fig. 4b). Since Nanoluc protein content in the EVs was similar (Supplementary Fig. S 4d), the overall increased signal after uptake indicated a generally improved release of all EV cargo molecules, not only the mRNA.

To test the effect of VSVg co-expression *in vivo*, mRNA EVs with and without VSVg were injected *in vivo* at an equal mRNA dose of 50 ng/kg body weight (n=4 per condition). Mice were sacrificed 24 h later, and the organs were analyzed for Nanoluc protein expression. Overall elevated Nanoluc protein signals, 5-fold for the kidney to 27-fold for the spleen, from all

analyzed tissue lysates were observed when VSVg was present on the injected EVs (Fig. 4c). This result indicated a successful increase in general EV cargo release by VSVg co-expression. Next, the performance of mRNA EVs (50 ng/kg body weight) compared to particle count-matched control EVs, both expressing VSVg, was tested *in vivo*. At 24 h post-injection, all analyzed organs from mice treated with mRNA-loaded EVs showed protein accumulation in comparison to organs from mice injected with control EVs (1.5-fold in the lungs to 3.7-fold in the liver), clearly demonstrating translation from EV-delivered, actively loaded Nanoluc mRNA (Fig. 4d). Taken together, these data show that the presence of VSVg strongly increases EV cargo delivery to recipient cells *in vitro* and *in vivo*. Therefore, by improving endosomal mRNA release, VSVg co-expression positively affects *in vivo* translation efficiencies of EV mRNA.

EV-delivered Cre recombinase mRNA induces genome editing *in vitro* and *in vivo*.
Although not problematic from a therapeutic perspective, in our described system the co-delivered passively loaded protein, Nanoluc, is very sensitive and may strongly mask the signal from newly translated protein derived from the delivered mRNA. To address this issue, we tested our EV mRNA loading platform by delivering Cre recombinase mRNA to cells stably expressing the Traffic Light Cre reporter system *in vitro* and *in vivo*. The Traffic Light reporter construct consists of a dsRed expression cassette flanked by loxP sites, followed by an in-frame eGFP coding sequence. The activity of Cre recombinase will lead to genomic recombination of the loxP sites, causing the deletion of the dsRed expression cassette, including the stop codon, and initiating the expression of the downstream eGFP cassette (Fig. 5a). Thus, the appearance of eGFP positive cells after addition of Cre recombinase protein or mRNA is unambiguously showing protein activity and functionality. We attempted the generation of Cre-PUFe$_{bind}$ mRNA stable cells, however, the integrated genomic cassette was repeatedly silenced and Cre mRNA expression was declining already after a few passages following selection. Therefore, Cre mRNA EVs were produced by triple co-transfection of plasmids encoding the Cre-PUFe$_{bind}$ mRNA, CD63-PUFe, and with or without VSVg, respectively (Fig. 5b). As established previously, passive loading-control EVs were produced by expressing the Cre-PUFe$_{bind}$ mRNA incompatible CD63-RBD fusion protein, CD63-MCP. The efficiency of genomic recombination in cells treated with control EVs, containing passively loaded Cre mRNA and protein only, served as baseline for assessing translation from actively loaded Cre-PUFe$_{bind}$ mRNA. After EV production and particle size validation (142.8 ± 12.9 nm (control), 132 ± 6.6 nm (PUFe), Supplementary Fig. S 5a), we measured Cre mRNA molecules in EVs by performing RT-qPCR on EV cDNA produced with or without RT. This allowed to determine the amount of Cre PCR template molecules derived from either residual plasmid or Cre mRNA (Fig. 5c and Supplementary Fig. S 5b). The active loading platform enriched mRNA EVs by about 0.5-1x10^4 molecules per 1x10^6 EVs as compared to control EVs, where no mRNA enrichment was detected. Next, two reporter cell lines with integrated Traffic Light cassette, B16F10 mouse melanoma and T47D human breast cancer cells, were treated *in vitro* with increasing amounts of EVs, corresponding to 0.3-30 pg per 10^4 cells of loaded Cre mRNA. Cells transiently transfected with plasmid served as positive control. In both cell lines, a dose- and time-dependent increase over 72 h in eGFP positive cell frequencies was observed, mediated by Cre mRNA EVs with VSVg (Fig. 5d and Supplementary Fig. S 5c). EGFP frequencies in T47D-Traffic Light cells treated with the higher dose of Cre mRNA EVs even exceeded the eGFP frequencies measured in transiently transfected cells, indicating the superior efficiency of EV-delivered mRNA (Fig. 5d). More striking, however, was the evident lack of genome editing when recipient cells were treated with passively loaded control EVs. This observation clearly ruled out any misleading effect from co-isolated residual transfection complexes. Moreover, it demonstrated negligible passive loading of Cre-PUFe$_{bind}$ mRNA and a very low Cre protein passive co-loading during EV biogenesis, as opposed to the Nanoluc

mRNA loading platform. In fact, an EV proteomics dataset acquired in our lab previously, showed that Cre protein overexpression in EVs producer cells does not lead to passive Cre protein loading into EVs (unpublished). Hence, Cre-mediated genome editing *in vitro* using the Cre mRNA loading platform was a result of EV-mediated active mRNA cargo transfer.
To extend our findings to an *in vivo* setting, the B16F10 Traffic Light malignant melanoma model was used to perform intratumoral injections of engineered EVs. After successful tumor engraftment, equal amounts of Cre mRNA EVs or control EVs, respectively with and without VSVg co-expression, were injected directly into the tumor tissue (n=3 to 4 animals per condition). At 48 h post-injection, mice were sacrificed, and paraffin-embedded tumor sections were analyzed for Cre-mediated genomic editing by fluorescence microscopy. Edited eGFP-positive tumor cells were detected only in tumors treated with EVs actively loaded with Cre-PUFe$_{bind}$ mRNA, independently from VSVg co-expression, while tumors injected with control-loaded EVs showed no detectable editing (Fig. 5e and Supplementary Fig. S 6). Thus, genomic editing only occurred in cells treated with Cre mRNA-loaded EVs, not in cells treated with passively loaded control EVs. These data clearly demonstrate the excellent performance of our mRNA loading platform in mRNA enrichment and delivery, supporting the versatility of engineered EVs as mRNA delivery vehicles.

DISCUSSION

Functional delivery of therapeutic mRNA faces major challenges, including unfavorable drug stability, immunogenicity, and inefficient delivery, leading to insufficient therapeutic mRNA abundance at the target site. The data presented here address these matters by combining the use of EVs as nature's very own nanoparticles with state-of-the-art synthetic biology strategies to develop a highly promising new platform for functional mRNA delivery. To maximize Nanoluc mRNA loading into EVs, a highly efficient EV sorting platform consisting of the EV-abundant tetraspanin CD63 fused to an engineered version of the high-affinity RNA-binding protein (RBD) PUF[32], termed PUFe, was designed. This was followed by an enhancement of Nanoluc mRNA stability by co-expressing PABPc, a protein shown to protect mRNA from degradation by binding to the polyA tail[45-47]. Although EV-mediated mRNA delivery was almost absent *in vitro*, mice injected with these EVs showed extrahepatic Nanoluc mRNA translation at doses as low as 20 ng/kg body weight. Another major obstacle in functional delivery of mRNA therapeutics is inefficient endosomal escape and could be the reason for inefficient *in vitro* delivery. Thus, to further improve our strategy, VSVg was incorporated into the EV membrane. VSVg is a viral protein naturally capable of fusing the viral envelope with endosomal membranes and has been used to enhance EV cargo delivery before[26,48]. With this modification, Nanoluc mRNA delivery was substantially improved *in vitro* as well as *in vivo*. Furthermore, to clearly prove the functional delivery of mRNA as opposed to passively co-loaded protein, we next applied the loading platform to produce Cre mRNA-loaded EVs largely devoid of co-loaded protein. Using the Traffic Light reporter system, a clear delivery of Cre mRNA, but not protein, both *in vitro* and *in vivo* was demonstrated, proving the functionality of our EV-based mRNA loading platform.
As demonstrated by the passive loading control throughout the study, mere overexpression of the target mRNA is not sufficient for effective endogenous mRNA loading into EVs. Instead, we and others implemented active endogenous loading strategies to enrich EVs for target mRNA[26,27,38,39]. However, most studies use producer cell engineering strategies based on transient co-transfection of the target mRNA-encoding plasmid. Though very effective, this approach leads to the potential co-isolation of transfection complexes containing the mRNA-encoding plasmid with the EVs and could thus cause misinterpretation of experimental results from functional studies[29-31]. Our approach, on the other hand, takes advantage of the non-viral stable genomic integration of the Nanoluc mRNA expression cassette using the ϕC31

integrase system[40,41], and thereby ensures that the target mRNA can only be delivered by EVs, and not residual transfection complexes. Consequently, the design of our strategy includes the use of a passive loading control produced under equal biological conditions from the same producer cells, thus allowing for the setting of accurate baselines for the co-delivery of passively loaded mRNA and protein.

The endogenous Targeted and Modular EV Loading (TAMEL) approach has first been introduced by Hung and Leonard in 2016[26] demonstrating CD63 fused to the MS2 coat protein (MCP) as best-performing strategy to load mRNA into EVs. Here, we showed by direct comparison that the mRNA loading efficiency of our scaffold CD63-PUFe exceeded the efficiency of CD63-MCP, indicating that the choice and design of the RBD influences the performance of the RNA loading platform. The same is certainly true for the EV sorting domain, as it determines the EV subpopulation that the cargo is sorted into. Therefore, even though our platform performed better than the previously published TAMEL approach for mRNA loading, the absolute molecule numbers per EV might still be too low for exerting clinically relevant effects. Thus, further improvements of the platform could be implemented by fusing other highly abundant EV proteins to PUFe, or even employing combinatorial approaches to engineer a multitude of EV subpopulations. Moreover, the amount and stability of target mRNA in the producer cell is a limiting factor to successful EV loading. Therefore, as exemplified for the MS2-MCP system, enhancing mRNA stability by specific sequence design of the UTRs is another viable option for further improvement of the system[42].

To address a substantial obstacle in therapeutic EV cargo delivery, efficient endosomal escape, we incorporated VSVg into the membrane of our engineered EVs. However, there are risks associated with the use of VSVg, mostly related to safety concerns due to its viral origin, and thus the implementation of alternative fusogenic proteins would be advantageous before further advancing this system towards clinical application.

The current state-of-the-art delivery vehicles for RNA therapeutics are synthetic lipid-based nanoparticles, such as LNPs. However, one major drawback of the use of synthetic LNPs is the inefficient delivery into extrahepatic tissues. Here, we showed EV-mediated extrahepatic mRNA delivery at a dose at least one order of magnitude lower than currently used for LNP-mediated mRNA delivery[36] (Fig. 3). In fact, superior RNA delivery efficiencies *in vivo* by EVs as compared to LNPs has been reported previously using different EV engineering strategies[19,49]. Therefore, our results are an indispensable addition to the drug delivery field demonstrating the exceptional versatility of EVs engineered with our loading platform as functional mRNA delivery vehicles.

METHODS

Cell culture

HEK293T, Huh7, T47D-Traffic Light, B16F10-Traffic Light cells were cultured in DMEM medium with high glucose, GlutaMAX and pyruvate (Gibco). The medium was additionally supplemented with 1% Anti-Anti solution (Gibco) and 10% fetal bovine serum (FBS, Gibco). Cells were cultured in a humidified atmosphere at 37°C and 5% CO_2. All cells were kept at low passages (< 15 passages) and high viability (> 90%).

Construct generation

All overexpression constructs (EV scaffold and mRNA) were codon-optimized to ensure optimal expression and bought from Thermo Fisher Scientific already cloned into their Thermo vector backbone. All constructs were subcloned into the pLEX vector backbone using EcoRI and NotI restriction enzymes for transfection-based EV production. For the generation of mRNA stable cells, mRNA constructs were transferred to the FC550A-1 backbone (System Biosciences) belonging to their ϕC31 integrase vector system using the same restriction sites.

Transient transfection

For large-scale transfections and EV production, HEK293T cells were seeded in 150-mm cell culture dishes or 10-layer cell factories one day prior to reach a confluency of 70% at the time of transfection. Cells were either transfected using PEI Max 40K (Polysciences) at a DNA:PEI ratio of 1:3 (w/w) or Lipofectamine 2000 (Thermo Fisher Scientific) at a DNA:Lipofectamine ratio of 1:2 (w/v). Transfection complexes were allowed to form in serum-free defined medium (OptiMEM, Gibco), and added dropwise to the cells. After 4 h, transfection medium was removed and changed to OptiMEM as EV production medium.

For small-scale plasmid transfections, cells were seeded at an appropriate amount in a multi-well plate one day prior to the time of transfection. When the cells reached a 70% confluency, transfection medium containing plasmid DNA and Lipofectamine 2000 at a ratio of 1:2 (w/v) was added to the culture medium. The cells were harvested at 24 h post-transfection for expression analysis.

ϕC31 integrase stable cell generation

HEK293T cells stably expressing mRNA constructs were generated using the ϕC31 integrase system (System Biosciences) according to the manufacturers protocol. Briefly, HEK293T cells were co-transfected with the donor vector FC550A-1 containing the mRNA of interest flanked by attB donor sites and the integrase vector FC200PA-1 encoding for the ϕC31 integrase enzyme using Lipofectamine 2000 Transfection reagent at a ratio of 1:4 (w/v DNA:Lipofectamine 2000). The transient expression of the enzyme leads to a single-copy non-viral transgene integration into the host cell genome by site-specific recombination of the attB sites from the donor plasmid with a pseudo attP site in the genome[40,41]. The integrated cassette also encodes for the puromycin resistance gene. 48 h after transfection, Puromycin (1 µg/ml) was added to the culture medium to select for successfully transfected cells. Selection was completed at 2 weeks post-transfection, and cells were analyzed for genomic vector integration and transgene expression. For culture, stable cells were kept in full growth medium constantly supplemented with Puromycin at a final concentration of 4 µg/ml.

EV production

Depending on the application, EVs were produced from cells cultured either in 150-mm cell culture dishes ($12x10^6$ cells/plate, 20 ml culture medium) or 10-layer cell factories ($4.5x10^8$ cells/factory, 600 ml culture medium). After transient transfection, all medium was removed and HEK293T cells were cultivated in serum-free OptiMEM (Gibco). After 48 h, conditioned medium was collected and subjected to one of our streamlined differential centrifugation and ultrafiltration protocols for EV isolation. Briefly, medium was spun at 700xg for 5 min to remove residual cells, then at 2,000xg for 10 min to remove cell debris. The centrifuged medium was then filtered through a polyethersulfone (PES) membrane filter with 0.22 µm pore size (TPP). The following concentration steps were chosen according to experimental conditions and medium volumes. For small scale volumes and many samples, filtered conditioned media were subjected to ultracentrifugation at 100,000xg for 90 min at 4°C. For large scale volumes and few samples, the conditioned medium was run through a hollow-fibre filter (D06-E300-05-N, MIDIKROS 65CM 300 K MPES 0.5 MM, Spectrum Laboratories) using a tangential flow filtration system (KR2i TFF System, Spectrum Laboratories) at a flow rate of 100 ml/min with a transmembrane pressure at 3.0 psi and shear rate at 3700/sec. After diafiltration with PBS, the eluate was reduced to approximately 40–50 ml and then concentrated using an Amicon Ultra-15 10 kDa molecular mass cut-off spin filter (Merck Millipore). Final EV preparations were kept in sterile filtered PBS for immediate use or sterile PBS-HAT buffer[50] for storage at -80°C.

Nanoparticle Tracking Analysis

Nanoparticle tracking analysis (NTA)[51,52] is based on the motion of sub micrometer-sized particles in solution (Brownian motion) and was used for quantifying the concentration and size distribution of particles in all EV samples. NTA was performed using the NS500 instrument equipped with the NTA 2.3 analytical software (NanoSight). After isolation, an aliquot of each EV sample was diluted in 0.22 µm filtered PBS between 1:500 to 1:5000 to achieve an appropriate particle count of between $2x10^8$ and $2x10^9$ per ml for the measurement. The camera focus was adjusted to make the particles appear as sharp dots. Using the script control function, five 30 s videos for each sample were recorded, incorporating a sample advance and a 5 sec delay between each recording. All recordings were done in light scatter mode at a camera level of 13-14. The analysis of all EV measurements was performed with constant software settings, screen gain at 10 and detection threshold at 7.

RT-qPCR

A defined amount of RNA (for EV RNA at least 40 ng, for cellular RNA at least 100 ng) was subjected to cDNA synthesis using the High-Capacity cDNA Reverse Transcription Kit (Thermo Fisher Scientific) and a 15-mer oligo-dT primer according to the manufacturer's protocol. Briefly, 10 µl of a 2X RT master mix consisting of ddH_2O, 2X RT buffer, 8 mM dNTPs, 20 µM oligo-dT primer and 50 U MultiScribe Reverse Transcriptase was mixed with 10 µl RNA and incubated for 10 min at 25℃ followed by 2 h at 37℃ in a thermocycler. The reaction was stopped by heating to 85℃ for 5 min. Depending on the initial RNA input, cDNA samples were diluted with ddH2O so that 1 µl cDNA corresponded to 2 ng RNA for EVs or 5 ng RNA for cells. Quantitative real-time PCR (qPCR) was performed using the PowerUp SYBR Green Master Mix (Thermo Fisher Scientific), a pre-formulated universal 2X master mix containing Dual-Lock Taq DNA polymerase for real-time PCR. Briefly, a 10 µl qPCR reaction was set up using 5 µl 2X master mix, forward primer at 200 nM final concentration, reverse primer at 200 nM final concentration, 1 µl cDNA and ddH2O. Samples and standards were measured in triplicates using the CFX96 Touch Real-Time PCR Detection System (BioRad). Cycling conditions were used as follows: 1. 50℃ for 2 min, 2. 95℃ for 2 min, 3. 95℃ for 15 s, 4. 62℃ for 1 min + plate read, 5. go to 3 for 39 more times, 6. 95℃ for 15 s, 7. melt curve from 60℃ to 95℃ (increment 0.5℃) for 5 s + plate read. The primer sequences were as follows: Nanoluc (Fw, 5'-TGAGGACTTCGTGGGTGACTG-3', Rev, 5'-CAAGACTATTCTCTGTATGGGCGT-3'), eGFP (Fw, 5'-CCCATTCTGGTGGAACTGGAC-3', Rev, 5'-GATGAACTTCAGGGTCAGCTTTC-3'), mOx40L (Fw, 5'-TCTAGACCTCGCTTTAAGTGGA-3', Rev, 5'-GGTCTTTCGCAGGGGAACT-3'), Cre (Fw, 5'-ATGAAGTGCGGAAGAACCTGATG-3', Rev, 5'-GGAACCACTTTCTGTTGTTCAGC-3'), GAPDH (Fw, 5'-ACATCGCTCAGACACCATG-3', Rev, 5'-TGTAGTTGAGGTCAATGAAGGG-3'). Primers were designed to amplify the 5'end of the respective mRNA, thus only full-length transcripts were quantified.

Relative and absolute quantification of RT-qPCR data

Full-length target mRNA in producer cells were measured using the $2^{-\Delta\Delta Cq}$ relative quantification method with GAPDH mRNA expression as reference.

As there is no validated reference mRNA for EV mRNA analysis established yet, we applied absolute quantification of Nanoluc mRNA molecules in RNA from EVs using standard curves with known molecular concentrations generated for each primer pair. Thus, we PCR-amplified the target product from an appropriate template, such as the expression plasmid or cDNA, using the HotStarTaq Plus Master Mix Kit (Qiagen) as follows: 1. 95℃ for 5 min, 2. 94℃ for 30 s, 3. Primer-defined annealing temperature for 30 s, 4. 72℃ for 1 min, 5. go to 2 for 30 more times, 6. 72℃ for 10 min. The PCR product was run on a 1% agarose gel and the correct band according to size was purified using the NucleoSpin Gel and PCR Cleanup kit (Macherey-Nagel) according to the manufacturer's protocol. The DNA concentration of the purified PCR product was measured using the NanoPhotometer NP80 (Implen) and diluted in a solution of

murine RNA at 2 ng/µl in a series of 10X-steps up to 10^{-9}-fold. The optimal range of standard dilution series was determined for each primer pair and usually observed between the 10^{-4} and 10^{-7} dilutions. For each assay of qPCR performed on sample cDNA derived from EV RNA or cellular RNA, at least 3 serial dilutions of the respective standard were analyzed on the same plate. The Cq values of the standards were correlated to their absolute molecule count per reaction as determined by the initial template concentration, amplicon length and molecular weight, and final dilution. For every primer pair a standard curve was calculated using linear regression. Then, the standard curve equation was applied to the samples. Apart from the Cq values measured and their quantification according to the standard curve, the calculations of absolute mRNA molecules in a sample included the total amount of isolated RNA, the RNA amount used in reverse transcription as well as the RNA amount corresponding to the cDNA per qPCR reaction. Lastly, the absolute molecules were normalized per cell or per $1x10^6$ EVs.

RNA transfection

Huh7 or HEK293T recipient cells were seeded at $1x10^5$ cells per well in a 24-well plate. The following day, 125 ng RNA purified from either EVs or corresponding producer cells were transfected per well in serum-free OptiMEM (Gibco) using Lipofectamine 2000 at a ratio of 1:2 (w/v), i.e. 0.25 µl per transfection. After 30 min incubation at room temperature, transfection complexes were added directly to the culture medium. Cells were harvested and lysed for protein measurement and Nanoglo luciferase assay at 3, 6, 12, 24, and 48 h post-transfection.

NanoGlo luciferase assay

The NanoGlo luciferase assay kit (Promega) was used to determine the amount of functional Nanoluc protein in lysed biological samples by supplying the enzyme with substrate and immediately measuring the resulting luminescence. To achieve this, cells were lysed directly in the well of the cell culture plate in an appropriate amount of PBS supplemented with 0.1% Triton-X100. Lysis was performed on ice for 30 minutes. Lysates were collected and cleared by centrifugation. The protein concentration was measured using the DC protein assay kit (BioRad) according to the manufacturers protocol.

Tissue samples from internal organs were weighed and suspended in 1 ml ice-cold PBS supplemented with 0.1% Triton-X100. Mechanical disruption was performed using the TissueLyser II and 8-mm stainless steel beads (both Qiagen) at an amplitude of 30 for 2 min at a time. After each lysis run, samples were rested on ice and viscosity was tested by pipetting up and down. Lysis steps were repeated as necessary until lysates were homogenous without obvious remains of solid tissue.

25 µl EVs, cell lysate, or diluted tissue lysate from murine internal organs were used for Nanoluc luciferase detection. The EVs or lysates were plated in opaque 96-well microplates. NanoGlo reagent (NanoGlo Luciferase Assay System, Promega) was prepared from NanoGlo lysis buffer and NanoGlo substrate solution according to the manufacturer's instructions. Using the GloMax 96 Microplate Luminometer (Promega), 25 µl NanoGlo reagent were added to each well by automatic injection and immediately analyzed.

EV uptake *in vitro*

For quantification of cellular uptake of Nanoluc-$PUFe_{bind}$ mRNA-loaded EVs *in vitro*, human hepatocellular carcinoma (Huh7) cells were seeded at a density of $6x10^4$ cells per well in a 24-well plate. The following day, the culture medium was renewed and EVs were added directly to the culture medium. Per test, equal amounts of EVs (mRNA-loaded or control), ranging from $1x10^8$ to $7.5x10^{10}$ per well, were used to eventually assess the excess Nanoluc protein signal of mRNA translation over pre-existent passively loaded protein. The corresponding doses of actively loaded mRNA ranged from 0.02 pg/10^4 cells ($1x10^8$ EVs without PABPc co-expression) to 14 pg/10^4 cells (with PABPc co-expression), depending on loading efficiencies

and scope of the experiment. EVs were co-cultured with the cells for 2 to 48 h, as indicated per experiment. Then, the EV-containing medium was removed, the cells were washed extensively in PBS (at least 3 times for 15 minutes each) by gentle horizontal shaking, followed by lysis on the plate with PBS-TritonX 100 (0.1%). Then, cell lysates and conditioned media was subjected to the NanoGlo luciferase assay as described. For every treatment an "EV only"-control well was included: a cell culture well without cells was equally treated with the corresponding amount of EVs and the signal from the medium served as normalization control to account for the total protein delivered by the EVs without translation.
For quantification of cellular uptake and activity of Cre-PUFe$_{bind}$ mRNA-loaded EVs *in vitro*, human T47D-Traffic Light and murine B16F10-Traffic Light cells were seeded in a 96-well plate at a density of $1x10^4$ cells per well. The following day, the cell culture medium was renewed and equal amounts of mRNA-loaded and control-loaded EVs, ranging from $1x10^8$ to $1x10^{10}$ EVs per well, were added to the cells. EVs were co-cultured with the cells for 24 to 72 h, as indicated. For analysis, EV-containing medium was removed, and cells were enzymatically detached to be measured by flow cytometry for the frequency and intensity of eGFP expression.

Flow cytometry

For flow cytometry analysis, cells were enzymatically detached using 0.05% Trypsin (Gibco) and collected in microtubes using an appropriate amount of full growth medium. The cells were spun down at 900xg for 5 min and resuspended in 100 µL of full growth medium or PBS supplemented with 2% FBS. If applicable, cells were stained with the appropriate amount of fluorescent antibody for 30 min in the dark at 4℃, washed with 1 ml PBS, spun down at 900xg for 5 min, and resuspended in 100 µL of full growth medium or PBS supplemented with 2% FBS. Cells were transferred to a 96-well V-bottom microplate (Sarstedt) for flow cytometry analysis using a MACSQuant Analyzer 10 instrument (Miltenyi Biotec). Dead cells were excluded from analysis via 4,6-diamidino-2-phenylindole (DAPI) staining and doublets were excluded by forward/side scatter area versus height gating. Analysis was performed using FlowJo Analysis Platform (BD Biosciences).
Flow cytometry antibodies used in this study: Invitrogen anti-mouse OX40L Monoclonal Antibody (OX89)-FITC, Thermo Fisher Scientific).

Animal experiments

All animal experiments were performed in accordance with the ethical permits B4-16 and B5-16 and designed to minimize the suffering and pain of the animals. 10-weeks old, female C57BL/6 mice were used for the animal work.
For Nanoluc-mRNA *in vivo* experiments, equal amounts of Nanoluc-PUFe$_{bind}$ mRNA-loaded or control EVs were systemically injected into the mice by different injection routes (intravenously or intraperitoneally) depending on maximum injection volume, particle concentration of the isolated EV preparation, and the requirement of the experiment. The mRNA doses per injection were determined by the amount of actively loaded Nanoluc-PUFe$_{bind}$ mRNA per EV as measured by RT-qPCR. The corresponding EV doses ranged from 2.5×10^{11} EVs to $1x10^{12}$ EVs per animal. Mice were sacrificed at indicated time points and selected internal organs (liver, kidney, lung, spleen) were harvested. Organs were directly submerged in 1 ml lysis buffer (PBS supplemented with 0.01% TritonX-100), weighed, and lysed as described above to be analyzed using the NanoGlo luciferase assay.
For intratumoral delivery of EV-loaded Cre-PUFe$_{bind}$ mRNA the B16F10 malignant melanoma model was used. Briefly, B16F10-Traffic Light mouse melanoma cells were implanted subcutaneously into female C57BL/6 mice. Tumors were grown over 7-10 days until they reached a palpable size. Then, equal amounts of EVs as determined by particle counts were injected directly into the tumor tissue. The mice were sacrificed 48 h after injection, tumors

were harvested, and embedded in paraffin. Sections with 5 µm thickness were prepared for IHC staining to evaluate eGFP expression.

IHC staining for tumor tissues

For IHC staining, the sections of tissues were fixed by incubating them at 65℃ for 1 h. Then, the slides were incubated for 20 min in 100% xylene for deparaffinization, followed by incubation in 100% ethanol (twice, 3 min each time), 95% ethanol (3 min), 70% ethanol (3 min), and 50% ethanol (3 min) for rehydration. After deparaffinization and rehydration, the slides were rinsed for 5 min with cold tap water before incubating them in citrate buffer, pH 6.0 (Sigma) for antigen retrieval. Next, the slides were washed with PBS (3 times, 5 min each time) and blocked with blocking buffer (Thermo Scientific) for 30 min at 37℃. Then, blocking buffer was removed and the sections were incubated with primary anti-GFP antibody (Abcam, ab290, 1:200 dilution) overnight to ensure optimal binding. The next day, the primary antibody was carefully removed, the slides were washed in PBS (3 times, 5 min each time). Then, the sections were incubated with secondary gt-α-rb IgG H&L antibody (Alexa Fluor® 488) (Abcam, ab150077, 1:500 dilution) for 30 min at 37℃. After removal of the secondary antibody, the sections were washed with PBS (3 times, 5 min each time) and mounted with ProLong™ Diamond Antifade Mountant with DAPI (Thermo Scientific). Finally, stained sections were sealed with nail polish and stored in the dark until taking images.

Fluorescence Microscopy

Widefield images of tumor tissues were acquired on a Nikon C2+ confocal microscope equipped with Plan Apo 20x objective with numerical aperture 0.75 (Nikon Instruments, Amsterdam, The Netherlands). The sample was excited and detected with appropriate excitation laser lines and emission filters and the fluorophores were imaged sequentially. Image processing was performed using Fiji[53]. Background from images was removed by adjusting brightness and contrast on sample with positive signal and settings were applied to the rest of the images.

Software

All cartoons were created using the BioRender online tool (publication licenses available upon request). Bar graphs and statistical analysis were done using GraphPad Prism software. Flow cytometry data was analyzed and visualized using the FlowJo Analysis Software (BD Biosciences). Images from fluorescence microscopy analysis were processed using Fiji[53].

ACKNOWLEDGEMENTS

The fluorescence microscopy in this study was performed at the Live Cell Imaging Core facility/Nikon Center of Excellence, Department of Biosciences and Nutrition at Karolinska Institutet (KI), Stockholm, supported by the KI infrastructure council.

AUTHOR CONTRIBUTIONS

S.E.A., J.N., J.H., D.G., and L.E. initiated this project. J.N., D.G., J.H., L.E. and X.L. designed the project and cloned the constructs. A.M.Z. and X.L. designed, performed, and analyzed most of the experiments. V.C.L., M.D.L., D.G., G.C., L.E., J.H., N.K., Z.N., G.Z., S.R. contributed to design, performance, and analysis of experiments. S.E.A. and V.C.L were in charge of the overall project lead and management. A.M.Z. wrote the manuscript that was reviewed and complemented by all authors.

COMPETING INTERESTS / INTELLECTUAL PROPERTY STATEMENT

The authors declare the following competing interests: This work was funded by Evox Therapeutics Ltd. S.E.A. is a co-founder, consultant, and stakeholder of Evox Therapeutics Ltd. J.N. and D.G. are consultants and stakeholders of Evox Therapeutics Ltd. V.C.L., M.D.L., L.E., and J.H. are current or former employees of Evox Therapeutics Ltd. This work is protected by patent families WO2019092145 and WO2020225392 owned by Evox Therapeutics Ltd.
Patent information WO2019092145: applicant – Evox Therapeutics Ltd; inventors – J.N., D.G., L.E., and J.H.; international application number – PCT/EP2018/080681; status – valid; covered aspect of manuscript – The nucleic acid therapeutics are loaded into EVs using inventive engineering protein and nucleic acid engineering strategies to enhance loading into EVs and to facilitate release of the nucleic acid cargo molecules inside target cells.
Patent information WO2020225392: applicant – Evox Therapeutics Ltd; inventors – V.C.L, A.M.Z., X.L., M.D.L., and L.E.; international application number – PCT/EP2020/062791; status – valid; covered aspect of manuscript – The nucleic acid therapeutics are loaded into EVs using inventive protein and nucleic acid engineering strategies which stabilize the cargo nucleic acids and enhance loading into EVs, thereby enhancing therapeutic activity of the cargo nucleic acid molecules half-life.
G.C, N.K., Z.N., G.Z., and S.R. declare no conflict of interest.

REFERENCES

1 Chaudhary, N., Weissman, D. & Whitehead, K. A. mRNA vaccines for infectious diseases: principles, delivery and clinical translation. *Nature reviews. Drug discovery* **20**, 817-838, doi:10.1038/s41573-021-00283-5 (2021).

2 Weide, B. *et al.* Direct injection of protamine-protected mRNA: results of a phase 1/2 vaccination trial in metastatic melanoma patients. *J Immunother* **32**, 498-507, doi:10.1097/CJI.0b013e3181a00068 (2009).

3 Sahin, U., Karikó, K. & Türeci, Ö. mRNA-based therapeutics--developing a new class of drugs. *Nature reviews. Drug discovery* **13**, 759-780, doi:10.1038/nrd4278 (2014).

4 Vallazza, B. *et al.* Recombinant messenger RNA technology and its application in cancer immunotherapy, transcript replacement therapies, pluripotent stem cell induction, and beyond. *Wiley Interdiscip Rev RNA* **6**, 471-499, doi:10.1002/wrna.1288 (2015).

5 Xiong, Q., Lee, G. Y., Ding, J., Li, W. & Shi, J. Biomedical applications of mRNA nanomedicine. *Nano Res* **11**, 5281-5309, doi:10.1007/s12274-018-2146-1 (2018).

6 Hwang, W. Y. *et al.* Efficient genome editing in zebrafish using a CRISPR-Cas system. *Nat Biotechnol* **31**, 227-229, doi:10.1038/nbt.2501 (2013).

7 Wang, H. *et al.* One-step generation of mice carrying mutations in multiple genes by CRISPR/Cas-mediated genome engineering. *Cell* **153**, 910-918, doi:10.1016/j.cell.2013.04.025 (2013).

8 Dowdy, S. F. Overcoming cellular barriers for RNA therapeutics. *Nat Biotechnol* **35**, 222-229, doi:10.1038/nbt.3802 (2017).

9 Baden, L. R. *et al.* Efficacy and safety of the mRNA-1273 SARS-CoV-2 vaccine. *New England journal of medicine* **384**, 403-416 (2021).

10 Anderson, E. J. *et al.* Safety and immunogenicity of SARS-CoV-2 mRNA-1273 vaccine in older adults. *New England Journal of Medicine* **383**, 2427-2438 (2020).

11 Polack, F. P. *et al.* Safety and Efficacy of the BNT162b2 mRNA Covid-19 Vaccine. *N Engl J Med* **383**, 2603-2615, doi:10.1056/NEJMoa2034577 (2020).

12 Cao, Y. & Gao, G. F. mRNA vaccines: A matter of delivery. *EClinicalMedicine* **32**, 100746, doi:10.1016/j.eclinm.2021.100746 (2021).

13 Zhang, Y., Sun, C., Wang, C., Jankovic, K. E. & Dong, Y. Lipids and Lipid Derivatives for RNA Delivery. *Chem Rev* **121**, 12181-12277, doi:10.1021/acs.chemrev.1c00244 (2021).

14 Murphy, D. E. *et al.* Natural or Synthetic RNA Delivery: A Stoichiometric Comparison of Extracellular Vesicles and Synthetic Nanoparticles. *Nano Letters*, doi:10.1021/acs.nanolett.1c00094 (2021).

15 Sadauskas, E. *et al.* Kupffer cells are central in the removal of nanoparticles from the organism. *Part Fibre Toxicol* **4**, 10, doi:10.1186/1743-8977-4-10 (2007).

16 Théry, C. *et al.* Minimal information for studies of extracellular vesicles 2018 (MISEV2018): a position statement of the International Society for Extracellular Vesicles and update of the MISEV2014 guidelines. *Journal of extracellular vesicles* **7**, 1535750-1535750, doi:10.1080/20013078.2018.1535750 (2018).

17 Wiklander, O. P. B., Brennan, M. A., Lotvall, J., Breakefield, X. O. & El Andaloussi, S. Advances in therapeutic applications of extracellular vesicles. *Sci Transl Med* **11**, doi:10.1126/scitranslmed.aav8521 (2019).

18 Kooijmans, S. A. A., de Jong, O. G. & Schiffelers, R. M. Exploring interactions between extracellular vesicles and cells for innovative drug delivery system design. *Advanced drug delivery reviews* **173**, 252-278, doi:10.1016/j.addr.2021.03.017 (2021).

19 Tsai, S. J. *et al.* Exosome-mediated mRNA delivery in vivo is safe and can be used to induce SARS-CoV-2 immunity. *Journal of Biological Chemistry* **297**, 101266, doi:10.1016/j.jbc.2021.101266 (2021).

20 Usman, W. M. *et al.* Efficient RNA drug delivery using red blood cell extracellular vesicles. *Nature communications* **9**, 2359, doi:10.1038/s41467-018-04791-8 (2018).

21 Zickler, A. M. & El Andaloussi, S. Functional extracellular vesicles aplenty. *Nature biomedical engineering* **4**, 9-11, doi:10.1038/s41551-019-0507-z (2020).
22 Corso, G. *et al.* Systematic characterization of extracellular vesicle sorting domains and quantification at the single molecule – single vesicle level by fluorescence correlation spectroscopy and single particle imaging. *Journal of extracellular vesicles* **8**, 1663043-1663043, doi:10.1080/20013078.2019.1663043 (2019).
23 Gupta, D. *et al.* Quantification of extracellular vesicles in vitro and in vivo using sensitive bioluminescence imaging. *Journal of extracellular vesicles* **9**, 1800222, doi:10.1080/20013078.2020.1800222 (2020).
24 Gupta, D. *et al.* Amelioration of systemic inflammation via the display of two different decoy protein receptors on extracellular vesicles. *Nature biomedical engineering* **5**, 1084-1098, doi:10.1038/s41551-021-00792-z (2021).
25 Liang, X. *et al.* Extracellular vesicles engineered to bind albumin demonstrate extended circulation time and lymph node accumulation in mouse models. *Journal of extracellular vesicles* **11**, e12248-e12248, doi:10.1002/jev2.12248 (2022).
26 Hung, M. E. & Leonard, J. N. A platform for actively loading cargo RNA to elucidate limiting steps in EV-mediated delivery. *Journal of extracellular vesicles* **5**, 31027, doi:10.3402/jev.v5.31027 (2016).
27 Kojima, R. *et al.* Designer exosomes produced by implanted cells intracerebrally deliver therapeutic cargo for Parkinson's disease treatment. *Nature communications* **9**, 1305, doi:10.1038/s41467-018-03733-8 (2018).
28 Wang, Q. *et al.* ARMMs as a versatile platform for intracellular delivery of macromolecules. *Nature communications* **9**, 960, doi:10.1038/s41467-018-03390-x (2018).
29 McCann, J. *et al.* Contaminating transfection complexes can masquerade as small extracellular vesicles and impair their delivery of RNA. *Journal of extracellular vesicles* **11**, e12220-e12220, doi:10.1002/JEV2.12220 (2022).
30 McConnell, R. E. *et al.* Transfection reagent artefact likely accounts for some reports of extracellular vesicle function. *Journal of extracellular vesicles* **11**, e12253-e12253, doi:10.1002/JEV2.12253 (2022).
31 Nordin, J. Z. Transfection reagents affect Extracellular Vesicle cargo transfer to recipient cells: The importance of appropriate controls in EV research. *Journal of extracellular vesicles* **11**, e12227-e12227, doi:10.1002/jev2.12227 (2022).
32 Abil, Z., Gumy, L. F., Zhao, H. & Hoogenraad, C. C. Inducible Control of mRNA Transport Using Reprogrammable RNA-Binding Proteins. *ACS synthetic biology* **6**, 950-956, doi:10.1021/acssynbio.7b00025 (2017).
33 Filipovska, A., Razif, M. F., Nygård, K. K. & Rackham, O. A universal code for RNA recognition by PUF proteins. *Nature chemical biology* **7**, 425-427, doi:10.1038/nchembio.577 (2011).
34 Wang, Y., Cheong, C.-G., Hall, T. M. T. & Wang, Z. Engineering splicing factors with designed specificities. *Nature methods* **6**, 825-830, doi:10.1038/nmeth.1379 (2009).
35 Haurwitz, R. E., Sternberg, S. H. & Doudna, J. A. Csy4 relies on an unusual catalytic dyad to position and cleave CRISPR RNA. *The EMBO journal* **31**, 2824-2832, doi:10.1038/emboj.2012.107 (2012).
36 Hou, X., Zaks, T., Langer, R. & Dong, Y. Lipid nanoparticles for mRNA delivery. *Nat Rev Mater* **6**, 1078-1094, doi:10.1038/s41578-021-00358-0 (2021).
37 Hall, M. P. *et al.* Engineered luciferase reporter from a deep sea shrimp utilizing a novel imidazopyrazinone substrate. *ACS chemical biology* **7**, 1848-1857 (2012).
38 Wang, Q. *et al.* ARMMs as a versatile platform for intracellular delivery of macromolecules. *Nature communications* **9**, doi:10.1038/s41467-018-03390-x (2018).
39 Yang, Z. *et al.* Large-scale generation of functional mRNA-encapsulating exosomes via cellular nanoporation. *Nature biomedical engineering* **4**, 69-83, doi:10.1038/s41551-019-0485-1 (2020).
40 Chalberg, T. W. *et al.* Integration specificity of phage phiC31 integrase in the human genome. *J Mol Biol* **357**, 28-48, doi:10.1016/j.jmb.2005.11.098 (2006).

41 Calos, M. P. The phiC31 integrase system for gene therapy. *Curr Gene Ther* **6**, 633-645, doi:10.2174/156652306779010642 (2006).
42 Li, W., Maekiniemi, A., Sato, H., Osman, C. & Singer, R. H. An improved imaging system that corrects MS2-induced RNA destabilization. *Nat Methods* **19**, 1558-1562, doi:10.1038/s41592-022-01658-1 (2022).
43 Kebaara, B. W. & Atkin, A. L. Long 3'-UTRs target wild-type mRNAs for nonsense-mediated mRNA decay in Saccharomyces cerevisiae. *Nucleic acids research* **37**, 2771-2778, doi:10.1093/nar/gkp146 (2009).
44 Karousis, E. D., Gypas, F., Zavolan, M. & Mühlemann, O. Nanopore sequencing reveals endogenous NMD-targeted isoforms in human cells. *Genome Biol* **22**, 223, doi:10.1186/s13059-021-02439-3 (2021).
45 Fatscher, T., Boehm, V., Weiche, B. & Gehring, N. H. The interaction of cytoplasmic poly(A)-binding protein with eukaryotic initiation factor 4G suppresses nonsense-mediated mRNA decay. *RNA* **20**, 1579-1592, doi:10.1261/rna.044933.114 (2014).
46 Fatscher, T. & Gehring, N. H. Harnessing short poly(A)-binding protein-interacting peptides for the suppression of nonsense-mediated mRNA decay. *Scientific reports* **6**, 37311, doi:10.1038/srep37311 (2016).
47 Silva, A. L., Ribeiro, P., Inácio, A., Liebhaber, S. A. & Romão, L. Proximity of the poly(A)-binding protein to a premature termination codon inhibits mammalian nonsense-mediated mRNA decay. *RNA* **14**, 563-576, doi:10.1261/rna.815108 (2008).
48 Zhitnyuk, Y. *et al.* Efficient mRNA delivery system utilizing chimeric VSVG-L7Ae virus-like particles. *Biochem Biophys Res Commun* **505**, 1097-1102, doi:10.1016/j.bbrc.2018.09.113 (2018).
49 de Jong, O. G. *et al.* A CRISPR-Cas9-based reporter system for single-cell detection of extracellular vesicle-mediated functional transfer of RNA. *Nature communications* **11**, 1113, doi:10.1038/s41467-020-14977-8 (2020).
50 Görgens, A. *et al.* Identification of storage conditions stabilizing extracellular vesicles preparations. *Journal of extracellular vesicles* **11**, e12238, doi:10.1002/jev2.12238 (2022).
51 Sokolova, V. *et al.* Characterisation of exosomes derived from human cells by nanoparticle tracking analysis and scanning electron microscopy. *Colloids and Surfaces B: Biointerfaces* **87**, 146-150, doi:10.1016/j.colsurfb.2011.05.013 (2011).
52 Dragovic, R. A. *et al.* Sizing and phenotyping of cellular vesicles using Nanoparticle Tracking Analysis. *Nanomedicine : nanotechnology, biology, and medicine* **7**, 780-788, doi:10.1016/j.nano.2011.04.003 (2011).
53 Schindelin, J. *et al.* Fiji: an open-source platform for biological-image analysis. *Nat Methods* **9**, 676-682, doi:10.1038/nmeth.2019 (2012).

FIGURES

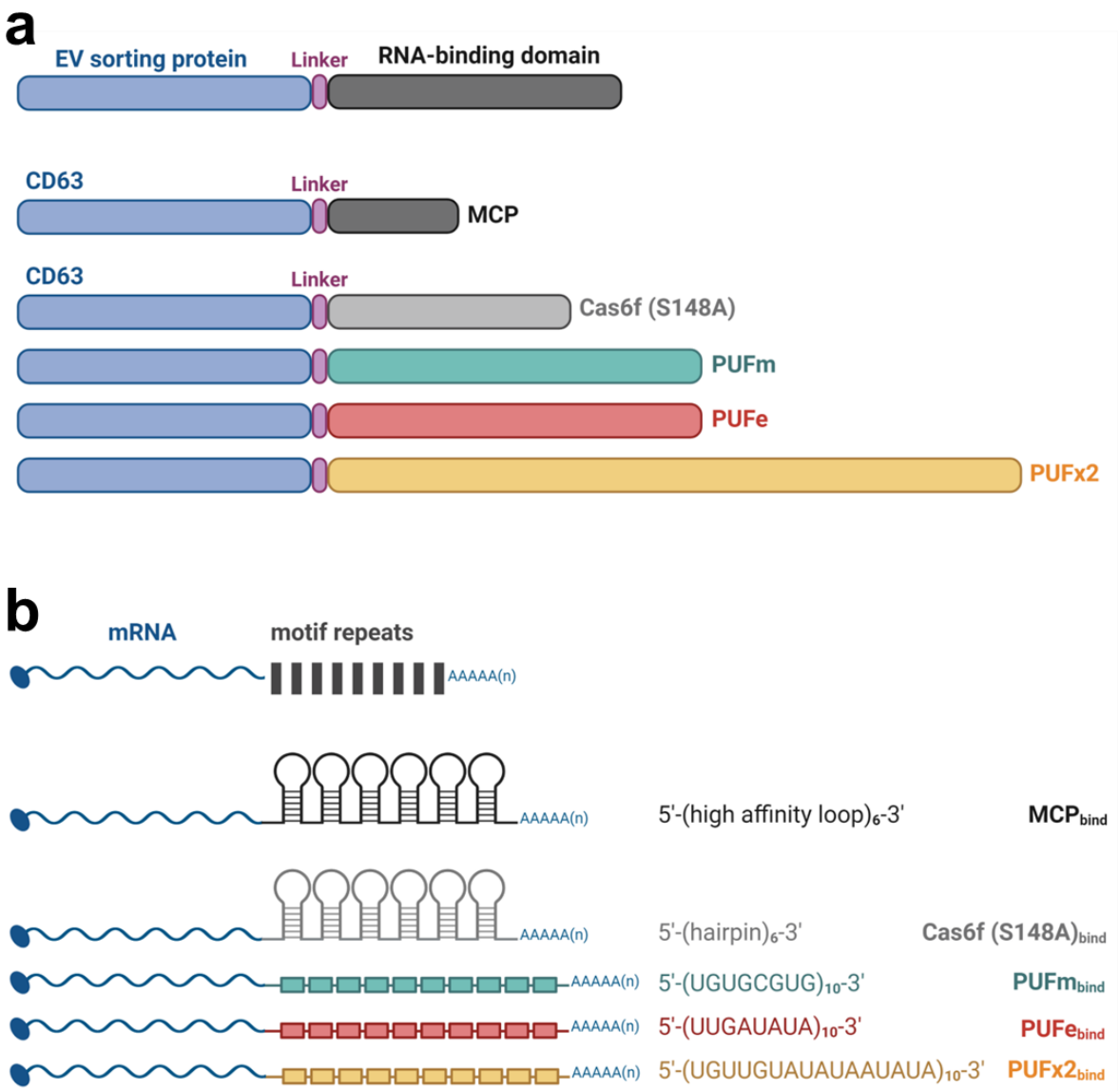

Fig. 1 Engineering strategy for endogenous mRNA loading into EVs. (a) EV sorting strategy: Four novel RNA-binding domains, the non-cleaving mutant Cas6f and three engineered versions of the designer Pumilio and FBF homology domain (PUF), termed PUFm, PUFe, and PUFx2, were fused via a glycine-rich linker peptide to the C-terminus of the EV sorting protein CD63. For performance comparison to a published platform, CD63-MCP (Hung et al) was included as well. (b) mRNA-binding strategy: mRNA coding sequences were codon-optimized and engineered to contain 6-10 repeats of the specific high-affinity motif recognized by the respective RNA-binding domain in their 3'UTR.

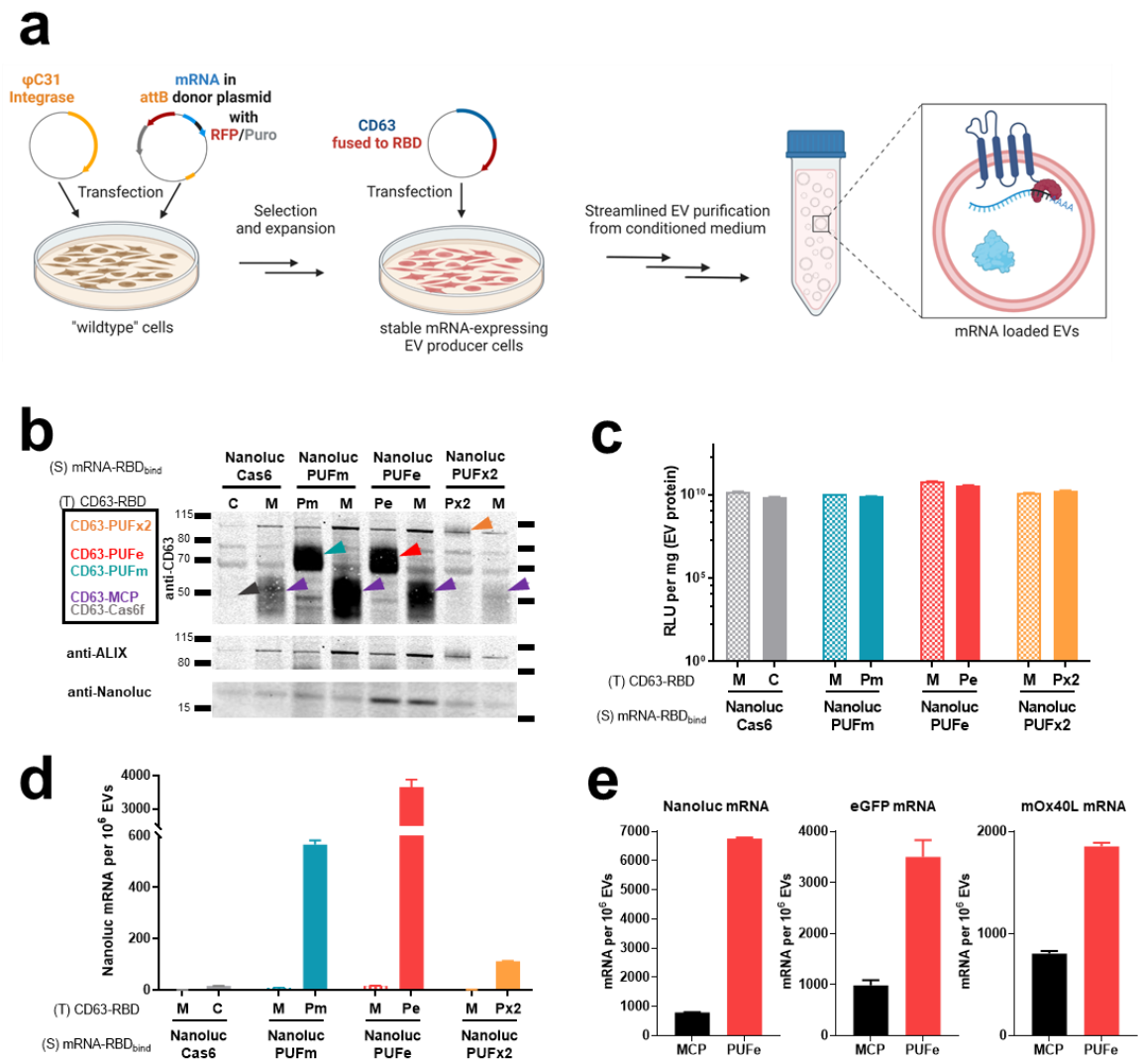

Fig. 2 Active mRNA loading into EVs from engineered mRNA single-stable producer cells. (a) Cartoon showing mRNA stable cell line generation using the ϕC31 integrase system, and subsequent EV production. For both mRNA EV and control EV production, the same mRNA stable EV producer cell line was used. Cells were either transiently expressing the compatible CD63-RBD (mRNA EVs) or the incompatible CD63-RBD (control EVs). This approach ensured the same biological pre-requisites during EV biogenesis for passive loading of engineered mRNA and protein. (b) Western Blot analysis of EVs produced from Nanoluc-RBD_{bind} (as indicated on top) mRNA stable EV producer cells. The expression of the EV protein-RBD fusion, either CD63-Cas6f (C), CD63-PUFm (Pm), CD63-PUFe (Pe), or CD63-PUFx2 (Px2), respectively, was validated by probing for CD63, sizes are indicated with colored arrowheads. To produce control EVs to account for passive loading of each engineered Nanoluc mRNA, incompatible CD63-MCP (M) was expressed in the respective producer cells. Moreover, expression of the EV marker ALIX and Nanoluc protein were detected. (c) Nanoglo luminescence assay to determine the amount of active Nanoluc enzyme per mg total EV protein in mRNA EVs (C, Pm, Pe, Px2) and control EVs (M) derived from Nanoluc-RBD_{bind} mRNA stable EV producer cells as indicated. (d) Absolute quantification by RT-qPCR of Nanoluc mRNA molecules per $1x10^6$ control EVs (M) or mRNA EVs (C, Pm, Pe, Px2) from one representative experiment. CD63-PUFe repeatedly showed superior performance in mRNA loading. (e) CD63-PUFe mediated EV mRNA loading as determined by RT-qPCR is superior to the published CD63-MCP platform for three different engineered mRNAs, Nanoluc, eGFP, and mOx40L. Shown here is one representative EV loading experiment for each mRNA. (T) – transient, (S) – stable, RLU – relative luminescence unit

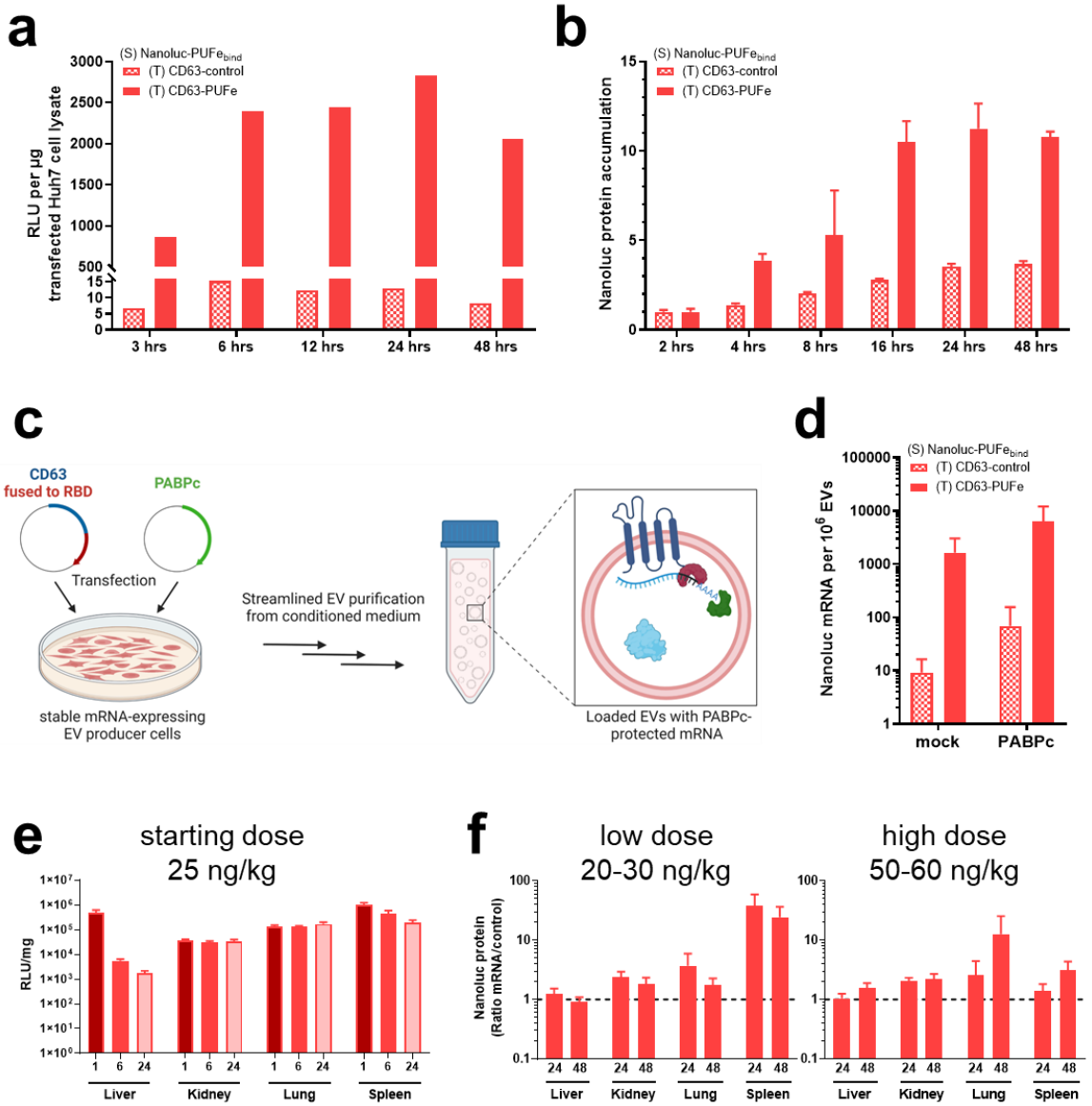

Fig. 3 Engineered EVs deliver loaded Nanoluc mRNA *in vitro* and *in vivo*. (a) Purified EV RNA from Nanoluc mRNA EVs and control EVs was transfected into Huh7 cells and Nanoluc protein activity was measured at indicated timepoints. RNA from mRNA EVs gave rise to high Nanoluc protein expression, proving functionality of EV-derived engineered mRNA in recipient cells. (b) Uptake of Nanoluc mRNA EVs at a dose of 0.6 pg Nanoluc mRNA per $1x10^4$ cells or particle count-matched control EVs in Huh7 recipient cells. Cellular Nanoluc protein activity was measured at indicated timepoints and normalized to the signal measured at 2 hrs, which corresponds to the signal from passively loaded Nanoluc protein. Uptake of Nanoluc mRNA EVs led to a substantially higher Nanoluc protein accumulation over time compared to control EVs, demonstrating EV-mediated engineered mRNA delivery and functional translation. (c) To enhance mRNA stability, EVs were produced while co-expressing PABPc in Nanoluc-PUFe$_{bind}$ mRNA stable producer cells. (d) PABPc co-expression had an advantageous effect on EV mRNA loading as quantified by RT-qPCR. (e) Nanoluc mRNA EVs with PABPc-stabilized mRNA were iv-injected into mice (n=3 per group) at 25 ng/kg body weight. Organs were analyzed for Nanoluc protein expression at 1, 6, and 24 h post-injection showing steady signal in kidney and lungs, indicative for extrahepatic EV delivery and mRNA translation. (f) Nanoluc mRNA EVs with PABPc-stabilized mRNA were iv-injected into mice (n=7 per group) at 20-30 ng/kg body weight and 50-60 ng/kg body weight in comparison to particle count-matched control EVs. Organs were harvested 24 and 48 h later, analyzed for Nanoluc protein activity, and values were normalized to respective control group values. A quotient of >1 revealed accumulation of Nanoluc protein, and thus mRNA translation.
(T) – transient, (S) – stable, RLU – relative luminescence unit

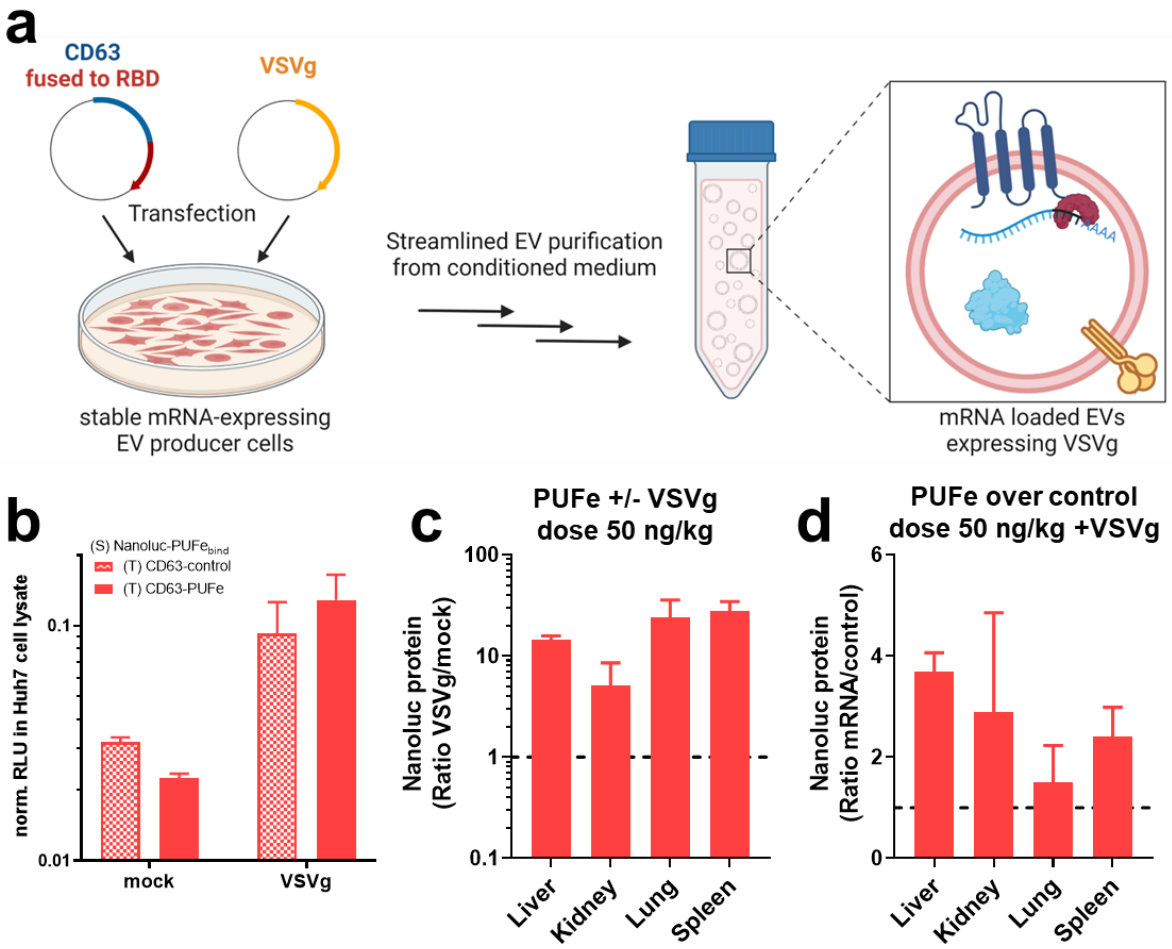

Fig. 4 Co-expression of the viral fusogen VSVg substantially increases EV cargo delivery. (a) Cartoon of VSVg co-expression in Nanoluc-PUFe$_{bind}$ mRNA stable EV producer cells, and subsequent EV production. (b) *In vitro* uptake analysis of Huh7 recipient cells treated with equal amounts of Nanoluc mRNA EVs at a dose of 0.2 to 0.3 pg mRNA per 1x10^4 cells, or particle count-matched control EVs, both with and without VSVg expression, respectively. Co-expression of VSVg on the EVs yielded higher Nanoluc protein signal in treated cells after 24 h, indicating a general improvement of EV cargo release and thus a beneficial effect on EV mRNA delivery. (c) Co-expression of VSVg enhances EV cargo delivery *in vivo*. Mice were i.p.-injected with Nanoluc mRNA EVs with or without VSVg co-expression at a Nanoluc mRNA dose of 50 ng/kg body weight (n=4 per group). Organs were analyzed for Nanoluc protein 24 h post-injection and data was normalized to signal obtained from animals injected with mRNA EVs at the same dose without VSVg. A quotient >1 indicated increased EV cargo delivery in the presence of VSVg, both for Nanoluc protein and mRNA. (d) Mice were i.p.-injected with Nanoluc mRNA EVs expressing VSVg at an mRNA dose of 50 ng/kg body weight, or particle count-matched control EVs expressing VSVg (n=4 per group). Organs were analyzed for Nanoluc protein 24 h post-injection, and the ratio of signal obtained from mice treated with Nanoluc mRNA EVs normalized on signal from mice treated from control EVs was consistently >1, showing extrahepatic translation.
(T) – transient, (S) – stable, RLU – relative luminescence unit

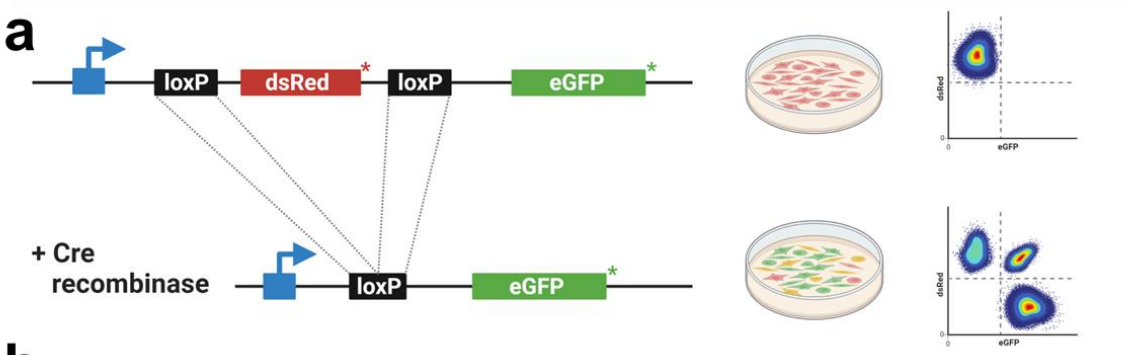
a
loxP
dsRed
loxP
eGFP
+ Cre recombinase
loxP
eGFP
dsRed
eGFP

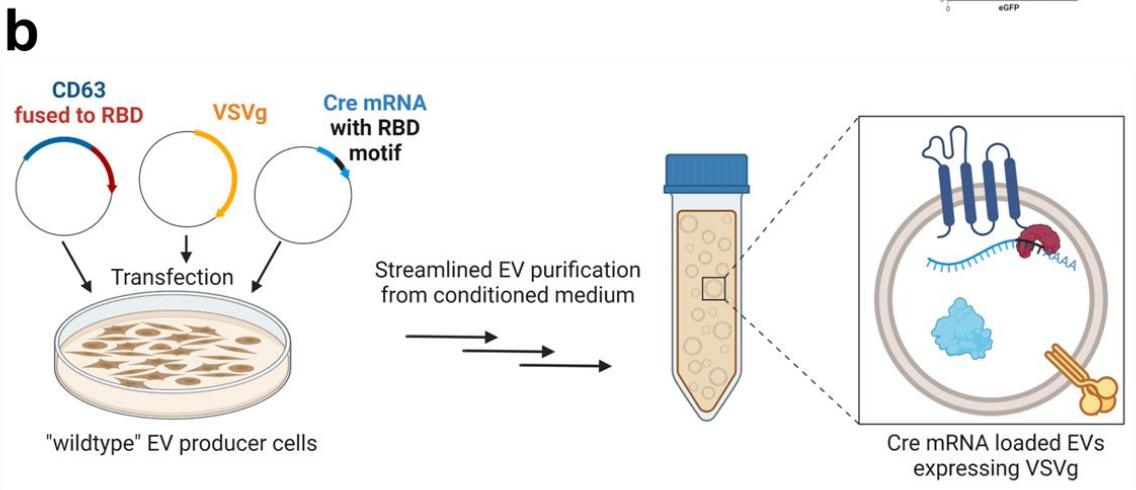
b
CD63 fused to RBD
VSVg
Cre mRNA with RBD motif
Transfection
"wildtype" EV producer cells
Streamlined EV purification from conditioned medium
Cre mRNA loaded EVs expressing VSVg

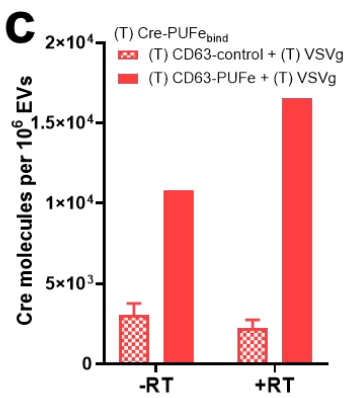
c
(T) Cre-PUFe bind
(T) CD63-control + (T) VSVg
(T) CD63-PUFe + (T) VSVg
Cre molecules per 10^6 EVs
2×10^4
1.5×10^4
1×10^4
5×10^3
0
-RT
+RT

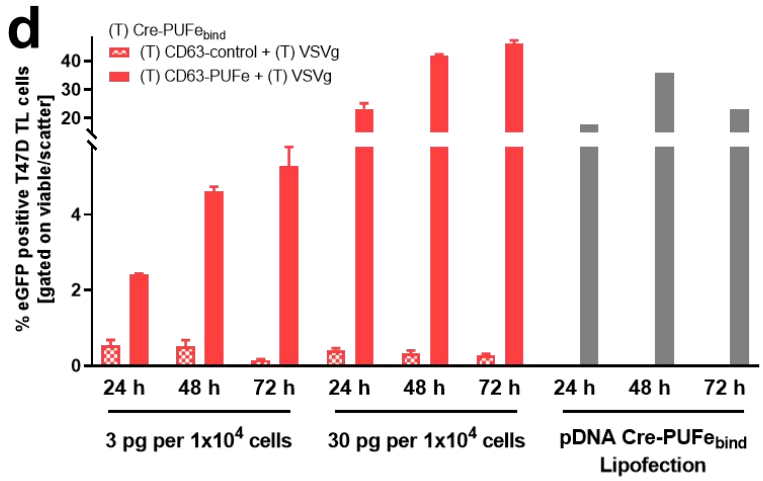
d
(T) Cre-PUFe bind
(T) CD63-control + (T) VSVg
(T) CD63-PUFe + (T) VSVg
% eGFP positive T47D TL cells [gated on viable/scatter]
40
30
20
4
2
0
24 h
48 h
72 h
24 h
48 h
72 h
24 h
48 h
72 h
3 pg per 1x10^4 cells
30 pg per 1x10^4 cells
pDNA Cre-PUFe bind Lipofection

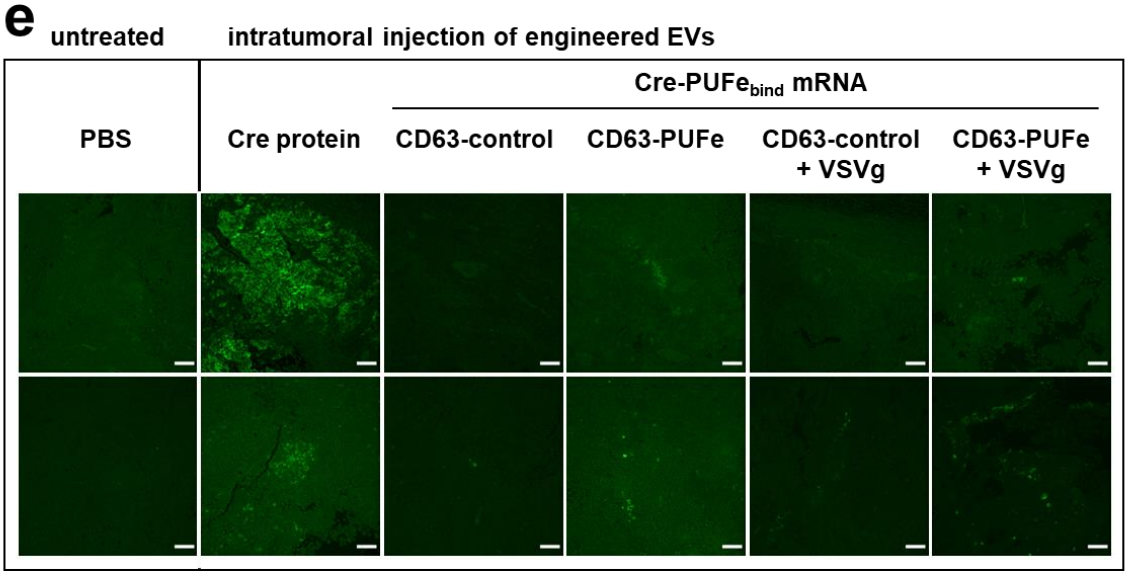
e
untreated
intratumoral injection of engineered EVs
PBS
Cre protein
Cre-PUFe bind mRNA
CD63-control
CD63-PUFe
CD63-control + VSVg
CD63-PUFe + VSVg

Fig. 5 EV-delivered mRNA encoding for Cre recombinase gives rise to functional protein *in vitro* and *in vivo*. (a) Scheme of the Traffic Light reporter system for Cre recombinase protein activity. Cre reporter cells stably express dsRed flanked by loxP sites, while an inactive, but in-frame, eGFP coding sequence is located further downstream. In presence of Cre recombinase, loxP sites recombine and the dsRed coding sequence is eliminated, resulting in active eGFP expression. A switch from dsRed to eGFP expression is thus evident for Cre recombinase protein functionality and genome editing and may be measured by flow cytometry. (b) Cre mRNA EVs or control EVs were produced by triple co-transfection of three plasmids, one encoding for Cre-PUFebind mRNA, one encoding for CD63-RBD (PUFe as compatible RBD or MCP as incompatible RBD) and one encoding VSVg or mock. Cre mRNA EVs from triple co-transfected producer cells carry actively loaded mRNA and VSVg for facilitated cargo delivery, while control EVs only contain passively loaded Cre mRNA and protein. (c) Nanoluc mRNA quantification in EVs. Quantitative PCR was performed on cDNA prepared without RT and with RT to assess the level of plasmid co-isolation in EVs. (d) T47D Traffic Light Cre reporter cells were treated with Cre mRNA EVs at increasing mRNA doses or particle count-matched control EVs for 24, 48, and 72 h. Expression of eGFP was measured by flow cytometry. Treatment with control EVs caused substantially less genomic editing in the reporter cells, validating very low passively loaded Cre mRNA and protein co-delivery as well as plasmid co-isolation. Transient transfection with plasmid DNA encoding for Cre-PUFe$_{bind}$ mRNA served as positive control. (e) B16F10 Traffic Light melanoma tumors were engrafted subcutaneously in mice and injected with Cre mRNA EVs or control EVs, with and without VSVg, respectively, PBS (negative control) or actively Cre protein-loaded EVs (positive control). Tumor sections were analyzed for eGFP expression at the injection site 48 h after injection by staining with anti-eGFP antibody. Edited tumor cells were only detectable in tumors injected with Cre mRNA EVs or Cre protein-loaded EVs. 20X magnififcation, scale bar 100 µm.